

Optimal modeling of end-mill spindle for improving the cutting stability

¹Jeevan Raju B, ²Rama Kotaiah K, ^{3*}Jakeer Hussain Shaik

Abstract

The prediction of the dynamic stability at the tip of the cutting tool is an essential factor in estimating the cutting stability of the machine tool at the design stage. In the present paper, an optimal design approach is presented to improvise the dynamic stability of the machining process. The integrated spindle-tool unit is initially analyzed with finite element modelling using the Timoshenko beam theory and the corresponding tool tip frequency responses are evaluated. In order to maximize the chatter-free regions in the stability lobe diagram (SLD), an optimization study is carried-out by considering spindle parameters such as bearing locations on spindle shaft along with tool-overhang as parametric design variables. Experimental simulations are carried out for the modelling data to arrive the output response parameters such as the fundamental frequencies and limiting average stable depth of cut for several combinations of the tool overhang and bearing span values with design of experiments (DOE). Analysis of variance and Taguchi's signal to noise ratios are used to estimate the influence on the response parameters. End-milling experiments are carried-out to validate the stability states corresponding to various axial depths of cut. Furthermore, the simulated data is generalized by using the feed-forward neural network model and it can be used as functional approximation. A global meta-heuristic optimization scheme namely genetic algorithm (GA) is employed to achieve the spindle design data corresponding to maximize the limiting stable depth of cut.

Keywords: Frequency response; spindle design; milling stability; lobe diagrams; parametric studies.

1. Introduction

High speed milling has made enormous technical tendencies recently. Enhanced spindle designs permit to supply the speeds up to 20krpm or even more in micro-milling. Greater metal removal rate may be received through machining at more axial depths of reduce and spindle speeds. However, a restriction to machining at more axial depths of leads to chatter phenomenon which causes the dynamic instability in machining generating insufficient

¹Research Scholar, Dept. of Mechanical Engineering, KLEF University, Vaddeswaram, India.

²Professor, Dept. of Mechanical Engineering, KITS Guntur, India.

^{3*}Associate Professor, Dept. of Mechanical Engineering, Malla Reddy Engineering College, Telangana, India. Corresponding Author: jakeershaik786@gmail.com

surface finish and maximum probably to wreck the tool and the machining work pieces. Motivated with the present needs of extraordinarily automatic manufacturing, the priority of

specific cutting forces and chatter mechanisms is specifically required to obtain the high volume of production with good quality machining. The stability lobe diagrams separate the stable and unstable cutting zones or accurately predict the chatter situations in the modern machining industries. Altintas and Budak (1995) confirmed the cutting force models, acquainted with the expectation steadiness in the stability lobes require the cutting force coefficients in the radial and axial directions, geometry of the tool etc. Several in advance works like Altintas and weck, 2004; Bravo et al., 2005; Gagnola et al., 2007; Tanga et al., 2009; dealt with the studies related to the research at the impact of milling method parameters on chatter. Suzuki et al. (2012) proposed a new method of identifying the tool tip transfer function with the inverse method and the chatter vibrations are evaluated. Raphael et al. (2014) developed a novel method to improve the accuracy of the stability of the lobe diagrams by the electronic spindle position and further reorganize the lobe diagrams. Very less works are identified which clearly dealt with the design principles of the milling spindles and related to other design factors and its responses at the tool tip are key factors to effectively plot the stability boundary diagrams are determined by are given by Lin and Tu, (2007); Jiang and Zhang, (2010); Penga et al., (2010); Cao et al., (2011); Gao and Meng, (2011).

Ozturk et al. (2012) identified the effect of the preload on the angular contact ball bearings and its combined effect on tool tip frequencies. Furthermore, the effect of the functional relationship between the spindle speed and bearing preload are tested with the experiments. Liu and Chen (2014) provided the constructive mathematical model for the estimation of the dynamic behaviour of the motorized high speed spindles. A flow chart related to the design parameters with sensitivity analysis is adopted for the system. Furthermore optimization studies are carried out by several authors by considering the several process parameters related to the end milling operation. Azlan et al. (2011) provided the numerical computing techniques such as the simulated annealing (SA) and validated with the genetic algorithm (GA) to obtain the better machining conditions and further these techniques are validated with the corresponding experiments. Jalili Saffar and Razfar (2010) portrayed a three dimensional model to predict the cutting forces for the end milling process at different conditions. Moreover, these predicted cutting forces were optimized with a genetic algorithm scheme and further validated with the cutting experiments. Palanisamy et al. (2007) implemented a new mathematical method to incorporate the effects of dynamics of machining as well as the material behaviour. A hybrid genetic algorithm technique was used to optimize the machining time during the machining process and minimize the tool vibration levels. Hsieh and Chu (2013) proposed an optimal tool path for the five-axis milling machine tool with a particle swarm optimization. Using the fully advanced PSO strategy the search capability of the algorithm has been enhanced to improve the tool path. Zarei et al. (2009) proposed the harmony search algorithm to work out the process parameters for the face milling operation. The overall machining cost has been reduced by optimizing the process parameters like spindle speed, feed rate and axial depth of cut.

In spite of these studies, very less works were identified in the literature which clearly defines the stability analysis with the utilization of the optimization techniques. Most of the studies

dealt with optimization of the process parameters but lacks in dealing with the geometric parameters as a function. In this work an attempt was made to study the optimized stability conditions of end milling process by considering few important modelling parameters of the integrated spindle unit with flexible body dynamics considerations. Using finite element modelling, the frequency response at the tip of the tool and the corresponding lobe diagrams are evaluated at various combinations of spindle bearing spans and overhang length of the tool. This correctness of these lobe diagrams from frequency responses is validated with few end-milling experiments on the existing spindle. This parametric data is employed to develop a function approximation task to correlate the geometrical design parameters with the average stable depth of cut by utilizing the feed forward neural network architecture. This neural trained model is employed to generate the function values for harmonic search optimization scheme resulting in an increasing the value of the average stable depth of cut. Further, the spindle is designed with the data obtained with respect to the bearing span and tool-overhang.

2. Modeling of the integrated spindle assembly

The vibration response of the spindle tool system is recognized by the means of the defined spindle tool system as shown in the Figure 1. All the segments of the spindle-tool system are discretized into five elements considering Timoshenko beam theory by including shear deformation and rotary deformation.

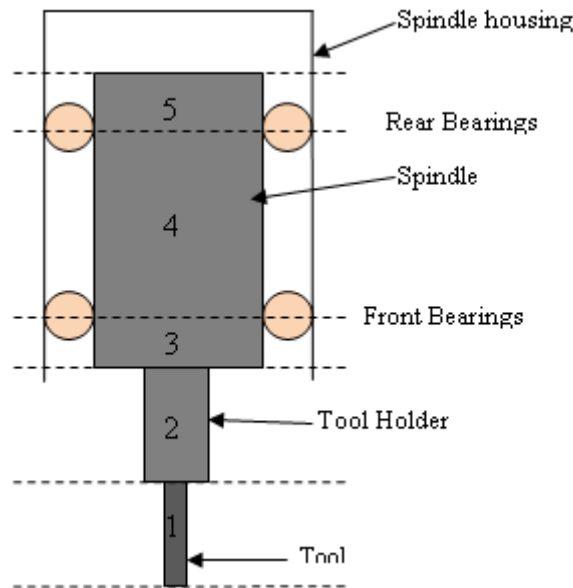


Figure 1. Equivalent model of spindle-tool device

The governing partial differential equations of the rotating spindle unit are:

$$\begin{aligned}
 \rho A(x) \frac{d^2 v}{dt^2} - \frac{\partial}{\partial x} \left[K_s A(x) G \left(\frac{\partial v}{\partial x} - \theta_z \right) - P \frac{\partial v}{\partial x} \right] - q_y - \Omega^2 \rho A(x) v &= 0 \\
 \rho A(x) \frac{d^2 w}{dt^2} - \frac{\partial}{\partial x} \left[K_s A(x) G \left(\frac{\partial w}{\partial x} + \theta_y \right) - P \frac{\partial w}{\partial x} \right] - q_z - \Omega^2 \rho A(x) w &= 0 \\
 \rho I \frac{d^2 \theta_y}{dt^2} + \Omega \rho J \frac{d \theta_z}{dt} - EI \frac{\partial^2 \theta_y}{\partial x^2} + K_s A G \left(\frac{\partial w}{\partial x} + \theta_y \right) - m_y &= 0
 \end{aligned}
 \tag{1}$$

$$\rho I \frac{d^2 \theta_z}{dt^2} - \Omega \rho J \frac{d\theta_y}{dt} - EI \frac{\partial^2 \theta_z}{\partial x^2} - K_s AG \left(\frac{\partial v}{\partial x} - \theta_z \right) - m_z = 0$$

where (u, v, w) are translational displacements in three different directions (x,y and z), $(m_x, m_y, \theta_y, \theta_z)$ are the moments per each length and rotations in the corresponding y and z direction, P is axial load on the beam, K_s is transverse shear form-factor, Ω is rotational speed, ρ is density, J is polar moment of inertia, G and E are shear and elastic modulus of the material. By modelling the restricted spindle rotation system the dynamics of the spindle tools unit can be well determined, as seen in Fig. 1. To model the spinning spindle, a two-node beam element incorporating the principle of Nelson's Timoshenko beam [16] with rotary inertia and shear deformation effect is used. It consists of five elements, six nodes and a complete of 28 degrees freedom is considered. Two angular ball bearings supported at the fourth and fifth nodes of the shaft. The cutting tool is expected is to be firmly attached to the spindle shaft tool holder. The complete equations within matrix form can be written by applying the Hamilton principle:

$$[M]\{\ddot{q}\} + [C] - \Omega[G]\{\dot{q}\} + ([K] - \Omega^2[M_c])\{q\} = F \quad (2)$$

Where the mounted mass, viscous damping and stiffness matrices $[K]$ are $[M]$, $[C]$ and $[K]$, the rotation speed is the $[G]$, whereas the word $[M_c]\{q\}$ implies a gyroscope matrix, the spring force's softening impact. Different ball bearings support the front and rear sections of the spindle shaft. The stiffness of angular contact covers depends on the loads applied and the layout of the covering. Several analytical formulas in the literature were suggested for measurement of the axial preload (F_a , ball diameter(D_b)) axial stiffness of the rollers, ball diameters(N_b), and contact angle of the static contact ball bearing(θ), and one of these were proposed.

$$k_{xx} = k_{yy} = 1.77236 \times 10^7 \times (N_b^2 \cdot D_b)^{1/3} \frac{\cos^2 \theta}{\sin^{1/3} \theta} F_a^{1/3} \quad \text{N/m} \quad (3)$$

With respect to above stiffness at the bearings the assembled real and imaginary portions of the FRF can explicitly be expressed as follows [15]:

$$[H(j\omega)] = [\text{Re}(\omega)] + j[\text{Im}(\omega)] = [-[M]\omega^2 + j\omega[[C] - \Omega[G]] + ([K] - \Omega^2[M_c])]^{-1} \quad (4)$$

Re and Im are the actual and imagination components of the spindle tool tip's frequency response feature.

Dynamics of Cutting Process

In the present paper, a two-dimensional cutting force model is used to represent the milling process to arrive at the cutting displacements in tangential and radial directions as shown in Fig 2

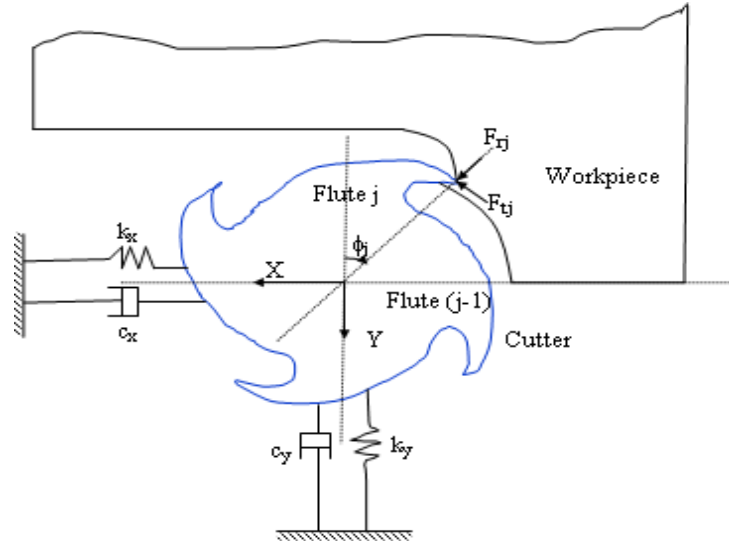


Figure 2. Two degrees milling model

The angular spindle speed is taken as Ω in rad/s, and the corresponding engagement with the time period (t) is taken as $\phi_j(t) = \Omega t$. In the radial direction, the total variable chip thickness is taken as follows:

$$h(\phi_j) = \{f_t \sin(\phi_j) + \delta x \sin(\phi_j) + \delta y \cos(\phi_j)\} * l(\phi_j) \quad (5)$$

Here the δx and δy are the relative displacements of the present and previous tooth periods. The cutting forces in the radial and tangential directions is represented as in terms of the chip thickness and axial depth of cut:

$$F_{r,j}(\phi) = \cos(\beta) K_s b h(\phi_j) = K_r b h(\phi_j) \quad (6)$$

$$F_{t,j}(\phi) = \sin(\beta) K_s b h(\phi_j) = K_t b h(\phi_j) \quad (7)$$

Further, the coefficients of cutting force in terms of specific force (K_s) and force angle (β) is taken as follows:

$$K_r = K_s \times \cos(\beta) \quad (8)$$

$$K_t = K_s \times \sin(\beta) = \left[\frac{K_s}{\sqrt{1 + K_r^2}} \right] \quad (9)$$

The local cutting forces acting on the tooth 'j' in the x-y system is represented as:

$$f_x = -F_t \cos(\phi) - F_r \sin(\phi) \quad (10)$$

$$f_y = F_t \sin(\phi) - F_r \cos(\phi) \quad (11)$$

The total cutting forces are arrived over the summation from tooth 'j' to ' N_t ' and are expressed as follows:

$$F_x(\phi) = \sum_{j=1}^{N_t} F_{x,j} \quad (12)$$

$$F_y(\phi) = \sum_{j=1}^{N_t} F_{y,j} \quad (13)$$

These total forces are expressed in the matrix form $[A(t)]$ and it depends on the angular position of the tool as follows:

$$\{F\} = \begin{Bmatrix} F_x \\ F_y \end{Bmatrix} = \frac{1}{2} b K_t [A(t)] \begin{Bmatrix} \Delta x \\ \Delta y \end{Bmatrix} \quad (14)$$

These expressions are periodic with the tooth pitch $\phi_p = \frac{2\pi}{N_t}$ (rad) and tooth period $\tau = \frac{60}{\Omega N_t}$

(s). These time-dependent forces are converted into the Fourier domain by accounting for the mean values as:

$$[A_0] = \frac{N_t}{2\pi} \begin{bmatrix} \alpha_{xx} & \alpha_{xy} \\ \alpha_{yx} & \alpha_{yy} \end{bmatrix} \quad (15)$$

Here the directional orientation factors is represented as:

$$\alpha_{xx} = \frac{1}{2} \left[(\cos(2\phi) - 2K_r\phi + K_r \sin(2\phi)) \right]_{\phi_s}^{\phi_e} \quad (16)$$

$$\alpha_{xy} = \frac{1}{2} \left[(-\sin(2\phi) - 2\phi + K_r \cos(2\phi)) \right]_{\phi_s}^{\phi_e} \quad (17)$$

$$\alpha_{yx} = \frac{1}{2} \left[(-\sin(2\phi) + 2\phi + K_r \cos(2\phi)) \right]_{\phi_s}^{\phi_e} \quad (18)$$

$$\alpha_{yy} = \frac{1}{2} \left[(-\cos(2\phi) - 2K_r\phi - K_r \sin(2\phi)) \right]_{\phi_s}^{\phi_e} \quad (19)$$

These above equations are again represented in terms of oriented frequency factors and the chatter frequency as:

$$\det([I] + \Lambda[H_o(i\omega_c)]) = 0 \quad (20)$$

Where $\Lambda = -\frac{N_t}{4\pi} b K_t (1 - e^{-i\omega_c \tau})$

The complex eigenvalue for equation (20) is considered in terms of cutting coefficients, chatter frequency, and immersional angles. The average depth of cut for a number of teeth (N_t) is evaluated as follows:

$$b_{\text{lim}} = -\frac{2\pi}{N_t K_t} \Lambda_{\text{Re}} (1 + \kappa^2) \quad (21)$$

Where $\kappa = \frac{\Lambda_{\text{Im}}}{\Lambda_{\text{Re}}} = \frac{\sin \omega_c \tau}{1 - \cos \omega_c \tau}$

The tooth passing period is expressed as $\tau = \frac{1}{\omega_c} (\varepsilon + \gamma 2\pi)$, here $\gamma=0, 1, 2, \dots$ is the number of

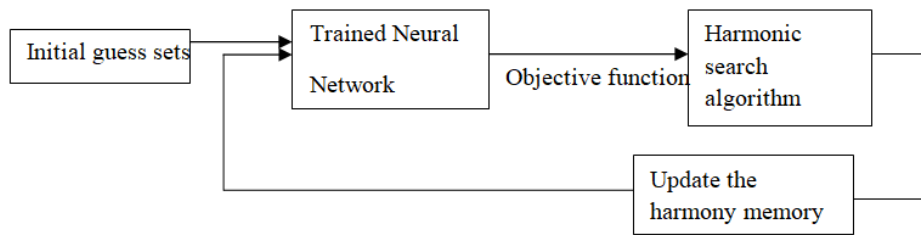
the lobes and phase shift is $\varepsilon = \pi - 2\mu$ and $\mu = \tan^{-1}(\kappa)$. Finally, the spindle speed in terms of tooth passing period and the number of teeth is expressed as follows:

$$\Omega = \frac{60}{N_t \tau} \text{ (rpm)} \tag{22}$$

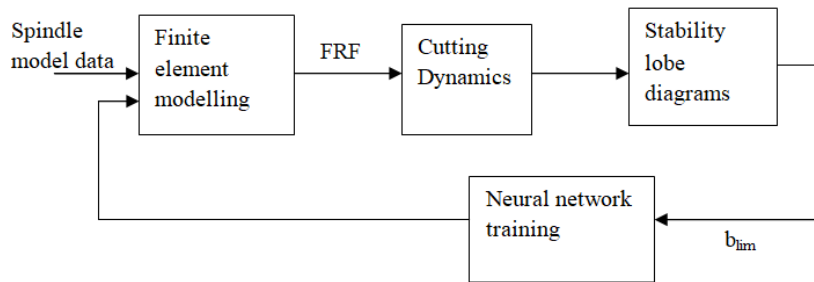
After arriving at the frequency responses at the tooltip, the stability lobe diagrams are plotted between the average stable depth of cut and spindle speeds.

Optimization Scheme

Using the modeling data of the spindle tool with respect to the design variables the corresponding stable depth of cut is optimized with the feed forward neural network by utilizing the trained data sets. Error back propagation algorithm with the updated weighted structure with a single layer model is employed for the system. To achieve the global optimum value several meta-heuristic algorithms like genetic algorithms, ant colony optimization, particle swarm optimization etc., are employed to get the solution. In this line, present work uses a similar latest scheme known as Harmony Search Optimization (HSO). Figure. 3(a) shows the adopted methodology for arriving the optimum process stability of end-milling process. The trained neural network is based on the design of experiments based on simulations as seen from Figure.3 (b) and the, weights obtained from the forward pass and the weights are stored separately. These weights are trained backwards and the average stable depth of cut is considered as the objective function. This function is utilized in the harmony search algorithm to get the optimal solution.



(a) Optimization scheme adopted



(b) Neural network modeling

Figure 3. Process flow chart for optimization

3. Results and Discussions

The spindle-tool data employed in the present task is listed in Table-1.

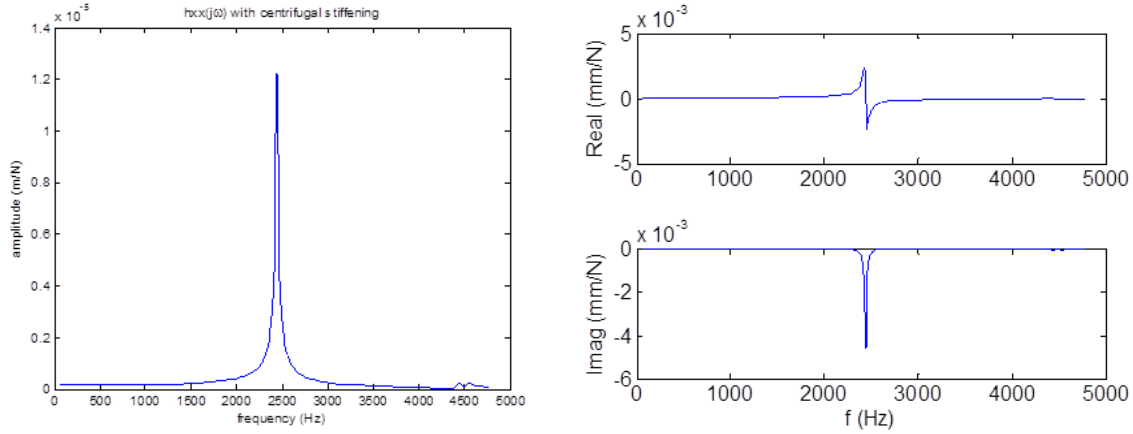
Table 1 Dimensions and properties of the spindle tool data

Parameters	Divisions of the elements				
	#1	#2	#3	#4	#5
Length(mm)	62	51	111	90	47
diameter(mm)	12	40	120	120	120

Optimal modeling of end-mill spindle for improving the cutting stability

E (Pa) 6.68×10^{11} 2.1×10^{11} 2.1×10^{11} 2.1×10^{11} 2.1×10^{11}

Figure. 4 represents the FRF obtained by considering material damping of 0.01, and the corresponding peak frequency is found to be at 2250Hz.

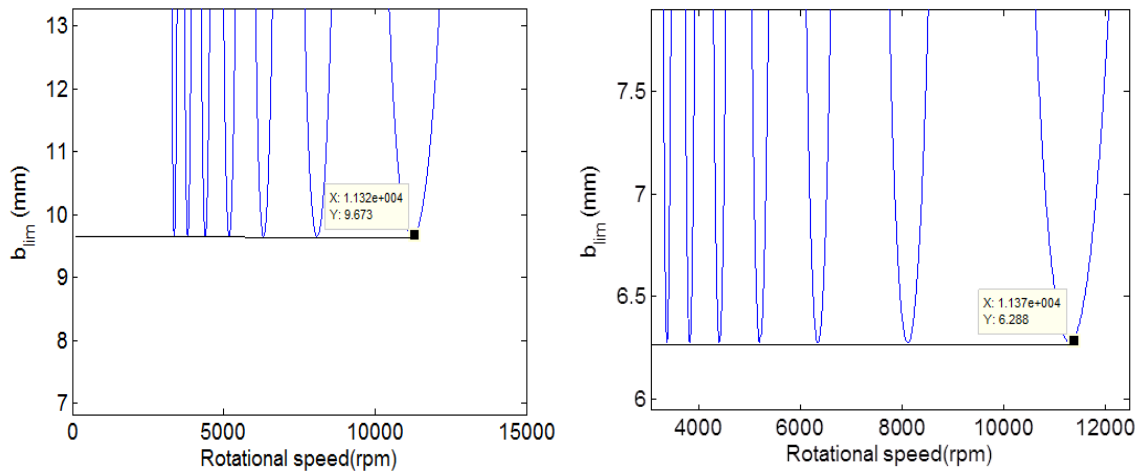


(a) Absolute tool tip FRF

(b) Real and imaginary parts

Figure 4. Tool tip frequency responses using the Full-order FEM

In order to obtain the stability lobe diagrams, the direction dynamic parameters employed are: cutting stiffness $K_{xx}=K_{yy}=2.1 \times 10^8$ N/m, tool diameter=19mm, helix angle of tooth (β) =68°, average specific cutting pressure (corresponding to Aluminum alloy) $K_s=750$ N/mm², teeth of the cutter =4, and damping ratios $\xi_x = \xi_y = 0.01$. Using the above machining data, the stability lobe diagrams are plotted with a down milling process various depths of radial immersions are shown in the figure 5. It is observed that, as there an increase in the radial immersion the average stable depth of cut increases.



(a) 30% Radial immersion

(b) 50% Radial immersion

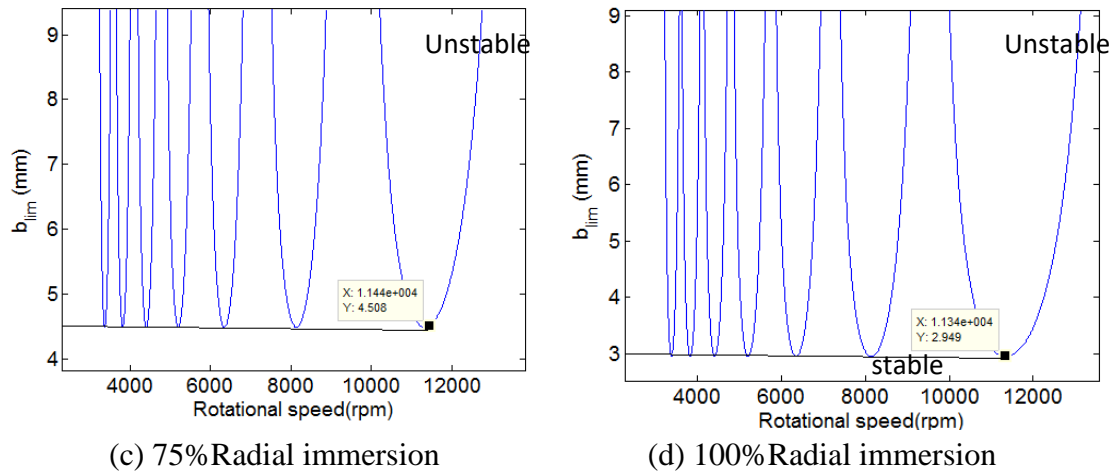


Figure 5. Stability lobe plots for different percentages of radial immersion

In the present work, the experimental cutting tests are conducted on the three axes CNC milling machine rotated at the same spindle speed as same considered in the for the numerical simulations. A High speed steel (HSS) milling cutter with four cutting edges with a diameter of 12mm is considered for the cutting tests and a full immersion with a down milling process is conducted on the aluminum alloy (Al6061). A four channel digital oscilloscope (DPO 43034) and an accelerometer with a frequency range of 1 to 10 KHz along with a charge amplifier are arranged in the required positions and are shown in the figure. 6

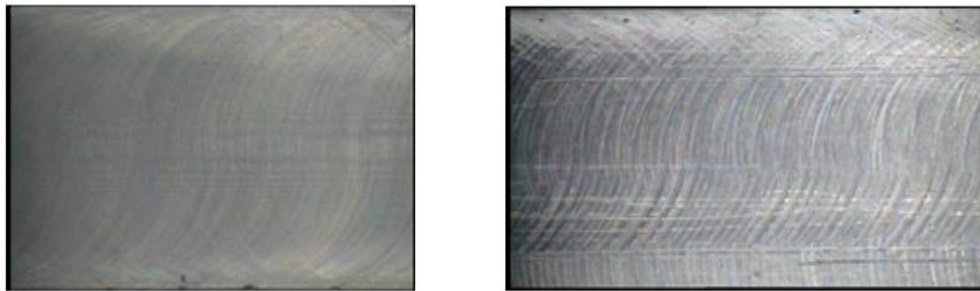


Figure 6. Experimental set up for the cutting tests

A series of cutting experiments are conducted on the CNC milling machine to validate the predicted stability lobe diagrams at the same cutting speeds and depths of cuts. The accelerometer is positioned at the non rotating portion of the spindle i.e at the housing portion with wax. Using this accelerometer, the cutting tool displacements are measured at various depths and spindle speeds. The amplitude of vibrations are enhanced with the help of charge amplifier and recored in the digital oscilloscope and further these data are utilised in the MATLAB platform to plot the response. The corresponding machining areas are photographed with help of the optical microscope at a magnification factor of 10X and the sample photos are shown in the figure. 7. It is idenfied that, as the depth of cut is at 0.07mm and a spindle speed of 2200 rpm the surface is having no chatter marks. As the depth of cut

Optimal modeling of end-mill spindle for improving the cutting stability

increases to more than 0.07 mm, the surface is prone to the chatter marks and is indicated with the clear picture in figure 7(b).

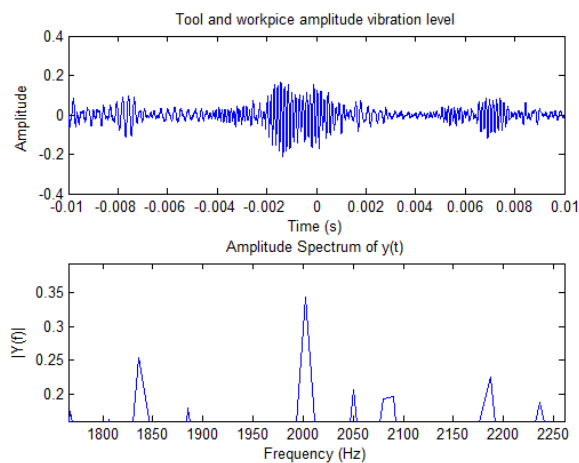


(a) Depth of 0.07mm

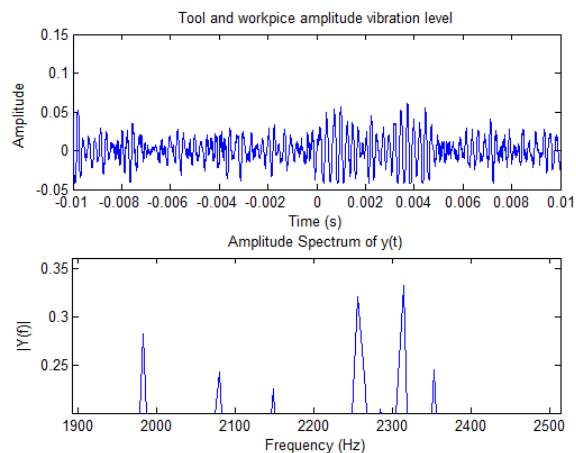
(b) Depth of 0.09mm

Figure 7. Machining areas of workpiece at different depths of cut

While the cutting tool progresses for the machining the tool displacements are measured with an accelerometer and are recorded in the time domain with the help of the oscilloscope. Figures 8(a) and 8(b) show the experimental FFT plots at the axial depths of 0.07mm and 0.09 mm. It is observed that the chatter frequencies are identified at the earlier frequencies as the depth of cut increases.



(a) Depth of cut 0.07mm



(b) Depth of cut 0.09mm

Figure 8. Amplitude plots for different axial depths of cut.

A series of cutting tests are conducted by considering the cutting points above and below the lobe diagram. The boundaries of the analytical stability lobe are verified by the optical surface images and as well as with the tool vibration levels. The corresponding points are interpolated in the lobe diagram with the circles and squares pertaining to the information related to the stable and unstable cutting zones as shown in the figure 9.

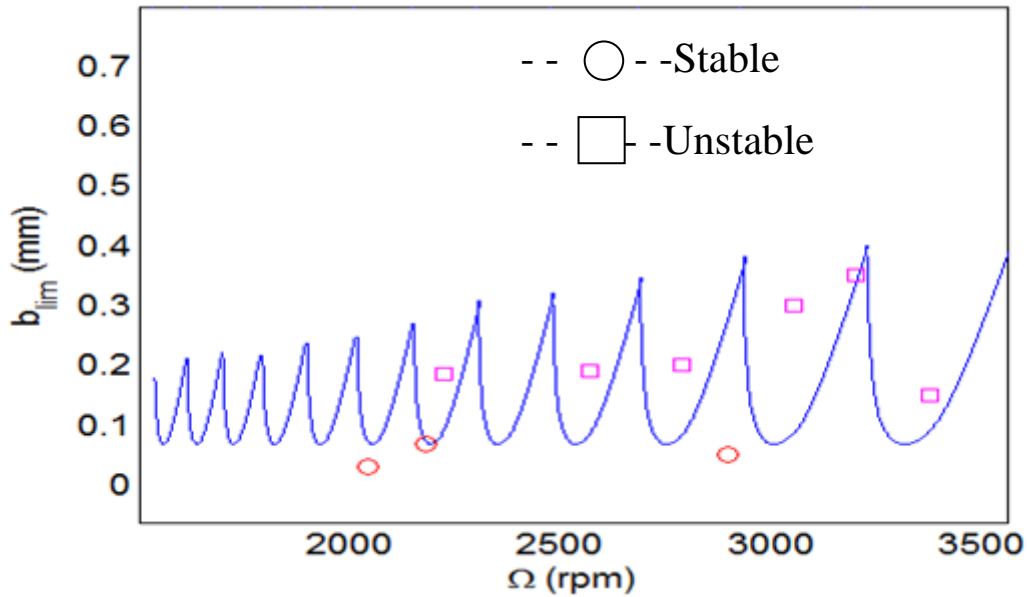


Figure 9. Predicted SLD with experimental validation

Optimum Design of Experiments

The first step before using the DOE is to know how many factors and levels. After identifying the number of factors and levels, orthogonal array is used to know the possible number of experiments. In order to reduce the numbers of experiments and maintain the resolution of the results, a five-level factorial design with two factors is implemented. Table-2 shows the process parameters and their levels for the experiments. Taguchi L25 (5**2) orthogonal array is used for the experimental design in order to predict the influence of controlled factors such as bearing span (BS), and tool overhang length(TO) on the output factors namely natural frequency (f) and average stable depth of cut (b). Here, the average depth of cut is predicted from the stability-lobe diagram over a range of operating speeds.

TABLE 2 Details of experiments conducted using Taguchi L₂₅(5**2) array.

Experiment Number	Tool overhang(TO) in mm	Bearing span(BS) in mm	First natural frequency(f) in Hz	Average stable depth of cut(b) in mm
1	75	90	1482.0	0.16110
2	75	150	1477.0	0.15960
3	75	210	1472.0	0.15760
4	75	270	1468.0	0.15720
5	75	330	1463.0	0.15450
6	90	90	1028.0	0.09623
7	90	150	1024.0	0.09464

Optimal modeling of end-mill spindle for improving the cutting stability

8	90	210	1020.0	0.09433
9	90	270	1019.0	0.09339
10	90	330	1017.0	0.09205
11	105	90	744.5	0.06374
12	105	150	739.5	0.06050
13	105	210	738.8	0.05900
14	105	270	735.6	0.05900
15	105	330	734.5	0.05300
16	120	90	549.7	0.04400
17	120	150	548.0	0.04100
18	120	210	544.9	0.04000
19	120	270	544.5	0.04000
20	120	330	543.5	0.03900
21	135	90	413.0	0.03200
22	135	150	407.3	0.03000
23	135	210	405.2	0.02800
24	135	270	404.7	0.02800
25	135	330	402.8	0.02800

Neural Network Based Optimization

In the current work, the most extensively used approach, the feed forward back propagation neural network, is designed for the prediction of natural frequencies and axial depths of cut for the end-milling operation. The numerically simulated data are passed forward from the input to output layer, calculated errors are propagated back order to update the weights. From various trails, neural network (NN) skeleton is chosen as shown in figure. 10.

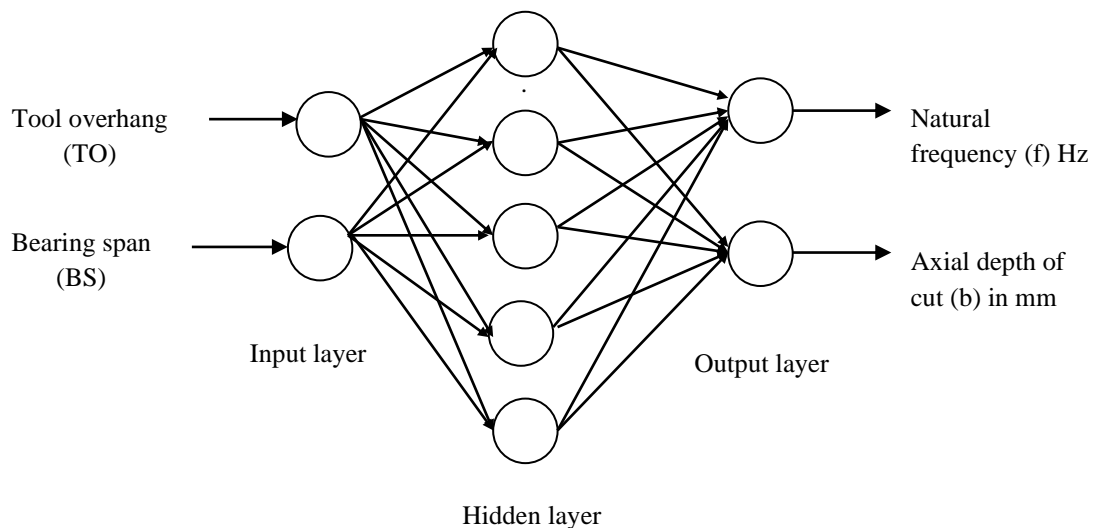


Figure 10. ANN model architecture

Here, bearing span (BS) and tool overhang (TO) are given as inputs and normalized values of natural frequency and average stable depth of cut are provided as target parameters. The natural frequencies (f) and average stable depths of cut (b_{lim}) can be predicted for any unknown input data containing bearing span and tool overhang of the system. A code is written in MATLAB to train the network and to acquire the weights. Figure.11 shows the convergence trend of trained neural data and the corresponding regression plot.

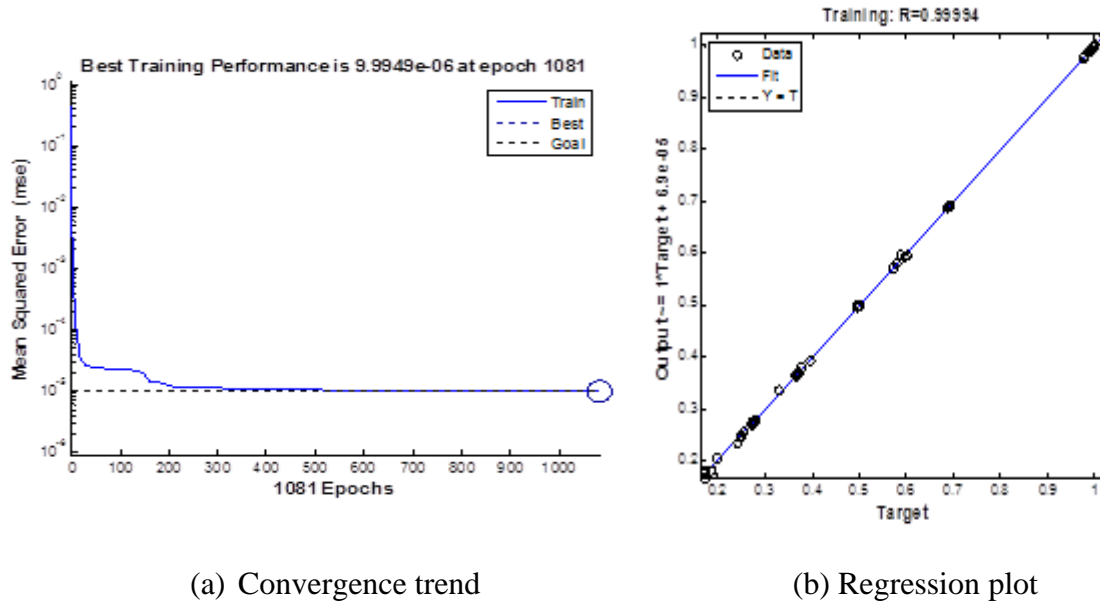


Figure 11. Neural network based training for design variables

In present work, using the model function derived from neural network, a modified harmony search optimization scheme is employed to maximize the stable depth of cut. In present simulations, a range of high and low values are taken based on the simulated data. The pitch adjustment rate(PAR) is taken as 0.1 to 0.5, harmony memory size(HMS)=6, harmony memory considering rate (HMCR)=0.8; range of variables for the tool overhang is taken as 60 to 140 and for the bearing span is taken as 90 to 380. The best optimal solution obtained for the range of variables for the tool overhang and bearing span as 110.55 and 240.3060. The modified HSO scheme is validated with the famous metaheuristic technique such as genetic algorithm with the same boundary conditions. It gives the following optimal values of 118.23 and 260.675. The following convergence pattern is observed in both GA and HSO techniques as shown in Figure 12.

Optimal modeling of end-mill spindle for improving the cutting stability

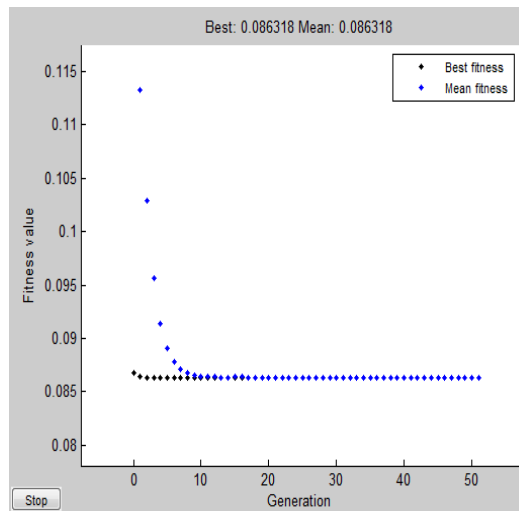


Figure 12. Error plot rate for the GA algorithm

Using these optimal design values, stability lobes are plotted as shown in figure. 13. It has been observed that modified HSO values gives a slight increase in average stable depth of cut indicated in blue colour lobe which has a depth of cut of 0.1235mm. While with the optimized values of GA indicated in magenta colour line has given an average stable depth of cut of 0.073mm. The best possible optimal values are possible to obtain using the modified HS algorithm compared with the GA technique.

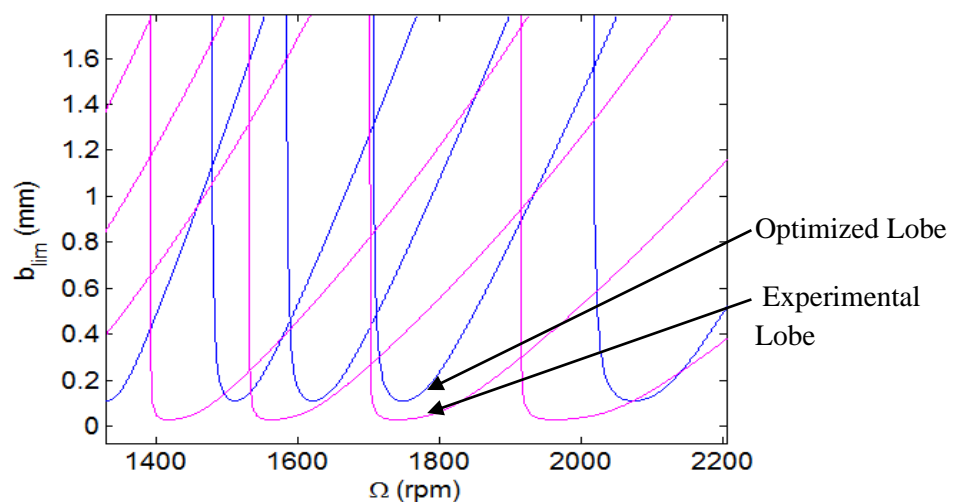


Figure 13. Stability lobe plots from design values GA and HS optimization.

4. CONCLUSIONS

In this paper a practical spindle model was considered for illustration and analyzed using finite element analysis by considering the effect of shear deformation and rotary inertia of spindle shaft. Initially, the stability lobes are plotted for different depths of radial immersion in down milling process. From the results it is arrived that when machining aluminium as the depth of immersion increases the axial depth of cut decreases. Although practically, machining of aluminium forms the built-up edges on the cutting tool at higher depths of cut. To avoid these effects a high percentage of radial immersion and high cutting speed is preferred which gives the stable machining. Experimental analysis proved that enhancement

in tool vibration levels causes the chatter marks on work piece beyond at a average stable of depth of cut of 0.07mm for slot milling. Later the parametric studies are conducted for different cases of bearing span and tool overhang for the spindle system and their influence on the system dynamics are considered and the corresponding stability lobes are plotted. It is observed that for large bearing span conditions the second mode of chatter frequencies have the considerable effect on the system dynamics which leads to produce the competing lobes which causes the dynamic instability during cutting conditions. The Taguchi's L25 orthogonal array is used for the design of experiments. An ANN model was developed and the results were generalized with the help of a feed-forward neural-network model so as develop a function approximation for the genetic algorithm to get the optimal values for the design variables.

REFERENCES

- Altintas, Y. (2000) Modeling Approaches and Software for Predicting the Performance of Milling operations at Mal-Ubc. *Machining Science and Technology: An International Journal*, 4:3445-478.
- Altintas, Y; Budak, E. (1995) Analytical prediction of stability lobes in milling. *Annals of the CIRP*, 44: 357-362.
- Altintas, Y; Weck, M. (2004) Chatter Stability of Metal Cutting and Grinding. *CIRP Annals- Manf.Tech*, 53:619-642.
- Bravo, U; Altuzarra, O; Lopez de Lacalle, L.N.; Sanchez, J.A.; Campa, F.J. (2005) Stability limits of milling considering the flexibility of the workpiece and the machine. *Int. J. Machine Tools & Manf*, 45:1669-1680.
- Briceno, J.F.; Mounayri, H; Mukhopadhyay, S. (2002) Selecting an artificial neural network for efficient modelling and accurate simulation of the milling process. *International Journal of Machine Tool and Manufacture*, 42:663-674.
- Cao, H; Holkup, T; Altintas, Y. (2011) A comparative study on the dynamics of high speed spindles with respect to different preload mechanisms. *Int. J. Machine Tools & Manf*, 57: 871-883.
- Fonga, T.Y.; Mingder, J. (2005) Dimensional quality optimisation of high-speed CNC milling process with dynamic quality characteristic. *Robotics and Computer-Integrated Manufacturing*, 21:506-517.
- Gagnola, V; Bouzgarrou, B.C.; Raya, P; Barra, C. (2007) Model-based chatter stability prediction for high-speed spindles. *Int. J. Machine Tools & Manf*, 47:1176-1186.
- Gao, S.H.; Meng, G. (2011) Research of the spindle over hang and bearing span on the system milling stability. *Arch Appl Mech*, 81:1473-1486.
- Hsieh, H.T.; Chu, C.H. (2013) Improving optimization of tool path planning in 5-axis flank milling using advanced PSO algorithms. *Robotics and Computer-Integrated Manufacturing*, 29:3-11.
- Jaberipour, M.; Khorram, E. (2010) Two improved harmony search algorithms for solving engineering optimization problems. *Commun Nonlinear Sci Numer Simulat*, 15: 3316-3331.

- Jakeer Hussain, S; Srinivas, J. (2013) Identification of dynamic rigidity for high speed spindles supported on ball bearings. *International Journal of Research in Engineering and Technology*, ISSN: 2319-1163 2(07):146-150.
- Jiang, S; Zheng, S. (2010) Dynamic Design of a High-Speed Motorized Spindle-Bearing System. *Journal of Mechanical Design ASME*, 132, 0345011-0345015.
- Lin, C.W.; Tu, J.F. (2007) Model-Based Design of Motorized Spindle Systems to Improve Dynamic Performance at High Speeds. *Journal of Manufacturing Process*, 9: 94-108.
- Liu, J; Chen, X. (2014) Dynamic design for motorized spindles based on an integrated model. *Int J Adv Manuf Technol*, 71:1961-1974.
- Mounayri, H; Briceno, J.F.; Gadallah, M. (2010) A new artificial neural network approach to modelling ball-end milling. *Int J Adv Manuf Technol*, 47:527-534.
- Mounayri, H; Kishawy, H; Briceno, J. (2005) Optimization of CNC ball end milling :a neural network -based model. *Journal of Materials Processing Technology*,166:50-62.
- Munoa, J; Dombovari, Z; Mancisidor, I; Yang, Y; Zatarain, M. (2013) Interaction Between Multiple Modes in Milling processes. *Machining Science and Technology: An International Journal*, 17:2:165-180.
- Ozturk, E; Kumar, U; Turner, S; Schmitz, T. (2012) Investigation of spindle bearing preload on dynamics and stability limit in milling. *Int. J. Machine Tools &Manf*, 61:343-346.
- Palanisamy, P; Rajendran,I; Shanmugasundaram, S.(2007) Optimizationofmachiningparametersusinggeneticalgorithmmandexperimentalvalidati onforend-millingoperations. *Int J Adv Manuf Technol*, 32:644-655.
- Penga, Z.K.; Jackson, M.R.; Guo, L.Z.; Parkin, R.M.; Meng, G. (2010) Effects of bearing clearance on the chatter stability of milling process. *Nonlinear Analysis: Real World Applications*, 11: 3577–3589.
- Raphael, G. S.; Reginaldo, T.C.(2014) A Contribution to Improve the Accuracy of Chatter Prediction in Machine Tools Using the Stability Lobe Diagram. *J. of Manf Science and Engg, ASME*, 136:021005-021007.
- Saffar, R. J.; Razfar, M. R.(2010) Simulation of end milling operation for Predicting cutting forces to minimize tool deflection by Genetic Algorithm. *Machining Science and Technology: An International Journal*,14:81-101.
- Suzuki, N; Kurata, Y; Kato, T; Hino, R; Shamoto, E. (2012) Identification of transfer function by inverse analysis of self-excited chatter vibration in milling operations. *Precision Engineering*, 36:568-575.
- Tanga, W.X.; Songa, Q.H. (2009) Prediction of chatter stability in high-speed finishing end Milling considering multi-mode dynamics. *Int. J. Machine Tools &Manf*, 209: 2585-2591.
- Xiang, W; qing, M; Li, Y; chun, R; Zhang, J. (2014) An improved global-best harmony search algorithm for faster optimization. *Expert Systems with Applications*, 41:5788–5803.
- Zain,A. M.; Haron, H; Sharif, S. (2011) Integration of simulated annealing and genetic algorithm to estimate optimal solutions for minimising surface roughness in end

milling Ti-6AL-4V. *International Journal of Computer Integrated Manufacturing*, 24:574-592.

Zareia, O; Fesanghary, M; Farshi, B; Saffar, J; Razfar R.M.R. (2009) Optimization of multi-pass face-milling via harmony search algorithm. *Journal of materials processing technology*, 209:2386-2392.

Zuperl, U; Cus, F; Reibenschuh, M. (2011) Neural control strategy of constant cutting force system in end milling. *Robotics and Computer-Integrated Manufacturing*, 27:485-493.